Journal of Hazardous Materials 219–220 (2012) 267–275

Contents lists available at SciVerse ScienceDirect

Journal of Hazardous Materials

journal homepage: www.elsevier.com/locate/jhazmat

Immediate and long-term impacts of potassium permanganate on photosynthetic activity, survival and microcystin-LR release risk of *Microcystis aeruginosa*

Huase Ou[a], Naiyun Gao[a,*], Chaohai Wei[b], Yang Deng[c], Junlian Qiao[a]

[a] State Key Laboratory of Pollution Control and Resources Reuse, College of Environmental Science and Engineering, Tongji University, Shanghai 200092, China
[b] College of Environmental Science and Engineering, South China University of Technology, Guangzhou 510006, China
[c] Department of Earth and Environmental Studies, Montclair State University, Montclair, NJ 07043, United States

ARTICLE INFO

Article history:
Received 29 September 2011
Received in revised form 3 April 2012
Accepted 3 April 2012
Available online 10 April 2012

Keywords:
Potassium permanganate
Cyanobacteria
Photosynthesis
Microcystis aeruginosa
Microcystin-LR

ABSTRACT

The immediate and long-term impacts of potassium permanganate ($KMnO_4$) as pre-oxidant on *Microcystis aeruginosa* and microcystin-LR (MC-LR) release risk were investigated. The cell density and the integrity of *M. aeruginosa* were determined by a flow cytometry, and typical photosynthetic parameters were measured by a pulse amplitude modulated fluorometer. The photosynthetic parameters were reduced to different degrees, accompanied with slight cytoclasis and complete degradation of extracellular MC-LR immediately after various dosages $KMnO_4$ oxidation (2–20 mg L^{-1}). In a 6-d cultivation following 5 mg L^{-1} $KMnO_4$ oxidation, the cell density decreased from 3.9×10^6 to 0.6×10^6 cells mL^{-1}, and then increased to 0.9×10^6 cells mL^{-1}, while the extracellular MC-LR increased from 0 to 51.2 μg L^{-1}. In the cultivation after 10 mg L^{-1} $KMnO_4$ treatment, the intracellular MC-LR and cell activity significantly declined, while significant cytoclasis (cell density from 3.8×10^6 to 0 cells mL^{-1}) and MC-LR release (increase from 0 to 15.2 μg L^{-1}) were observed. The photosynthetic parameters were found to be useful tools to predict the recovery tendency of *M. aeruginosa* cells, and the MC-LR release risk should be considered during $KMnO_4$ pre-oxidation in water-treatment plants.

1. Introduction

Nowadays, cyanobacterial blooms have increasingly occurred in various water sources and became a global problem [1]. Cyanobacteria are of particular concern for their ability to produce a large number of diverse secondary metabolites, which have negative impacts on water treatment processes. Certain cyanobacterial species can produce harmful microcystins (MCs) which have acute poisoning and chronic cancer promotion potentials to animals and human beings [2]. Moreover, some metabolites are undesirable odor and taste-causing compounds [3]. Furthermore, accompanied with the death of cyanobacteria during the pretreatment in water treatment plant, the residues and excretion are released into water and increase the level of natural organic matters those are well-known precursors of disinfection by-products [4]. Therefore, removal of cyanobacterial cells and their metabolites from raw water is an essential strategy to prevent the cyanobacteria-induced water quality degradation issues in water treatment.

Over the past decades, efforts had been made to evaluate effective technologies to address the removal of the cyanobacterial cells and their metabolites in drinking water treatment [5–7]. Traditional water treatment processes were proven to have limited efficiency for cyanobacteria removal, and unicellular cyanobacteria could penetrate through treatment facilities due to their small size (diameter < 10 μm). This might result in undesirable presences of cyanobacteria and metabolites in the finished water [8,9]. Thus advanced oxidation technologies were widely used to improve the cyanobacteria removal in water treatment plants [10]. Particularly, potassium permanganate ($KMnO_4$) pretreatment is effective on taste and odor controlling and biological growth prevention. It can also promote the coagulation [11] and control the production of disinfection by-products [12,13]. Furthermore, $KMnO_4$ was found to be a feasible option for MCs removal during pre-oxidation processes [14]. Chen et al. used $KMnO_4$ to degrade MC-RR and found that the second-order rate constant of reaction ranged from 0.154 to 0.225 L mg^{-1} min^{-1} at room temperature [15].

Since $KMnO_4$ exhibits as a temperate oxidant in natural heterogeneous waters (pH ≈ 7), cyanobacteria might still survive after practical $KMnO_4$ pretreatment. There is an urgent need to estimate the activity and integrity of cyanobacterial cells during $KMnO_4$ oxidation. As autotroph species, cyanobacteria rely on energy conversion using oxygenic photosynthetic systems, similar to plants and algae. The important photosynthetic apparatuses involve photosystem II (PS II), photosystem I reaction centers and phycobilisome [16]. The monitoring of these basic apparatuses can

* Corresponding author at: Mingjing Building, Tongji University, 1239# Siping Road, Shanghai 200092, China. Tel.: +86 21 65982691, fax: +86 21 65986313.
E-mail address: naiyungao@yahoo.com.cn (N. Gao).

0304-3894/$ – see front matter © 2012 Elsevier B.V. All rights reserved.
http://dx.doi.org/10.1016/j.jhazmat.2012.04.006

provide useful information about the activity of cyanobacteria. In practice, photosynthesis is so delicate that the oxidative stress and other environment conditions can easily disrupt the transfer of energy and mass. Thus, $KMnO_4$ oxidation might have negative effects on the activity of photosynthesis, resulting in death of cyanobacterial cells.

Currently, there is a lack of systematic studies, which have evaluated the effect of $KMnO_4$ on the activity and integrity of toxic *Microcystis aeruginosa* and the accompanying release risk of microcystin-LR (MC-LR). In the past decades, several researches have documented that pulse amplitude modulation (PAM) fluorometry provided an excellent representation of the activity of cyanobacteria [16,17]. Thus, it can be anticipated that PAM will explain the intrinsic mechanisms of $KMnO_4$ induced inactivation. In this study, for the first time, PAM and flow cytometry were used to investigate the immediate and long-term impacts of $KMnO_4$ on the activity and integrity of *M. aeruginosa*. We conducted cultivated experiments to assess the capacity of survive and recovery of *M. aeruginosa* after $KMnO_4$ treatment. Considering that the acute toxicity of MC-LR, its degradation and releasing risk in the cultivation were also estimated.

2. Materials and methods

2.1. Microorganisms and reagents

A toxic strain of *M. aeruginosa* (FACHB-912) was purchased from Institute of Hydrobiology, Chinese Academy of Sciences (Wuhan, China). This strain was cultivated in batch cultivation using BG11 medium in 1 L conical flasks. The incubator temperature was maintained at 25 °C and illuminated by ~30–40 μmol photons m^{-2} s^{-1} tubular fluorescent lamps with a 12-h diurnal cycle. All the reagents and solvents were analytical grade. Solutions were prepared using ultrapure water produced by a Gradient water purification system (Millipore, USA). The stock solution of $KMnO_4$ was prepared by dissolving crystal $KMnO_4$ (Sigma–Aldrich, USA) in Milli-Q water and filtered by 0.2 μm membrane filter (MFS, Japan). Then it was standardized to 1 g L^{-1} by titration with sodium oxalate. To quench the oxidation, sodium sulfite stock solution was prepared by dissolving certain amount of crystal sodium sulfite (Sigma–Aldrich, USA) in Milli-Q water (10 g L^{-1}) and filtered by 0.2 μm membrane filters (MFS, Japan).

2.2. $KMnO_4$ oxidation experiments

The *M. aeruginosa* cultivations were harvested in their growth exponential phase and diluted by BG11 medium to ~4.0×10^6 cells mL^{-1}. *M. aeruginosa* cell density was determined by a YS100 microscope (Nikon, Japan) using hemacytometer counting method and by a CytoSense flow cytometry (CytoBuoy, Netherlands). Prior to experiments, the solution pH was adjusted to 7 using phosphate buffer solution (KH_2PO_4–NaOH). In $KMnO_4$ oxidation experiments, predetermined volume of stock $KMnO_4$ solution was added to *M. aeruginosa* suspension. After 2 h of contract time under slow mixing with a magnetic stirrer, predetermined volume of sodium sulfite stock solution was added to quench the reactions. Then 15 mL sample was harvested for immediate PAM and flow cytometry analyses, while 20 mL sample was collected for intracellular and extracellular MC-LR analyses. Furthermore, 200 mL suspension was collected and cultivated in the same condition mentioned in Section 2.1 after a designated dosage $KMnO_4$ exposure. A 10 mL sample was obtained daily from cultivated samples for PAM analyses. Another 30 mL sample was harvested for flow cytometry and MC-LR analyses every two days.

2.3. Sample analyses

To acquire three *in vivo* parameters with the PHYTO-PAM phytoplankton analyzer (Walz, Germany), 5 mL suspension sample was immediately analyzed after harvesting. While the sample is acclimated to the light of its environment, the photosynthetic parameter Φ_e can be calculated as:

$$\Phi_e = \frac{\Delta F}{F_{m'}} = \frac{F_{m'} - F_s}{F_{m'}} \quad (1)$$

where F_s and $F_{m'}$ are the corresponding light-acclimated steady-state and maximum fluorescence, respectively [18]. The other two photosynthetic parameters (α and $r\mathrm{ETR}_{\max}$) were calculated following the methods described by Ralph and Gademann [19]. In practice, these parameters all can be obtained directly from PHYTO-PAM analyzer. For flow cytometry analyses, 10 mL sample was obtained and then fixed by formaldehyde solution (38%, Sigma, USA) to a final concentration with 4% formaldehyde. Measurement parameters were designated following the method described by Thyssen et al. [20]. The samples were measured by flow cytometry and the raw data included cell density, fluorescence red (FLR) responsivity data set and forward scattering (FWS) responsivity data set. Cell density can be automatic counted by CytoClus3 (CytoBuoy, Netherlands) and the other two data signal sets can be parameterized into 8 numerical entities by CytoClus3 to extract the shape information from the cells (detailed information can be seen at http://www.cytobuoy.com/). The FLR responsivity was obtained directly from the sub parameter "maximum amplitude" of the FLR signal set with a unit of mV, while the average cell diameter was obtained from the sub parameter "particle length" of the FWS signal set with a unit of μm. Scatter diagrams of flow cytometry data were plotted using Origin (Microcal, USA).

For MC-LR determination, 20 mL of original suspension was separated in a centrifuge (CT15RT, Techcomp, China) at 10,000 rpm for 10 min, and the supernatant was filtered with 0.7 μm GF/F glass-fiber filter (Whatman, UK) to obtain the extracellular MC-LR contained solution (Fraction A). Thereafter, the glass-fiber filter with cyanobacterial cells was shredded into pieces and diluted together with the centrifugal sediment by ultrapure water to form the diluted cyanobacterial cells suspension. The diluted cyanobacterial cells suspension was treated to break the cells in an ultrasonic cell disintegrator (250A, Branson, USA) with a power of 300 W for 3 min. Subsequently, the ultrasound-treated suspension was centrifuged and filtered as done previously, to eventually obtain the intracellular MC-LR contained solution (Fraction B). The intracellular MC-LR solution was diluted with the ratio of 1:100 while the extracellular fraction was diluted with the ratio of 1:50. Both fractions were determined using a microcystin enzyme-linked immunosorbent assay (ELISA) kit purchased from Institute of Hydrobiology, Chinese Academy of Sciences (Wuhan, China) [21]. The detection range of ELISA kit is 0–4 μg L^{-1} and the detection limit is 0.05 μg L^{-1}. For statistical treatment, the analysis was performed with three replicates. Two-way ANOVA analysis conducted in SPSS 19.0 was used to validate the significant differences among control and treated samples.

3. Results

3.1. Immediate impairment of photosynthetic capacity

Three photosynthetic parameters, including the effective quantum yield (Φ_e), photosynthetic efficiency (α) and maximum electron transport rate ($r\mathrm{ETR}_{\max}$), were measured immediately subsequent to different dosages $KMnO_4$ treatments (Fig. 1). Φ_e is an approximation to the fraction of absorbed energy used for photochemistry in the total energy at a specific time, thus it is

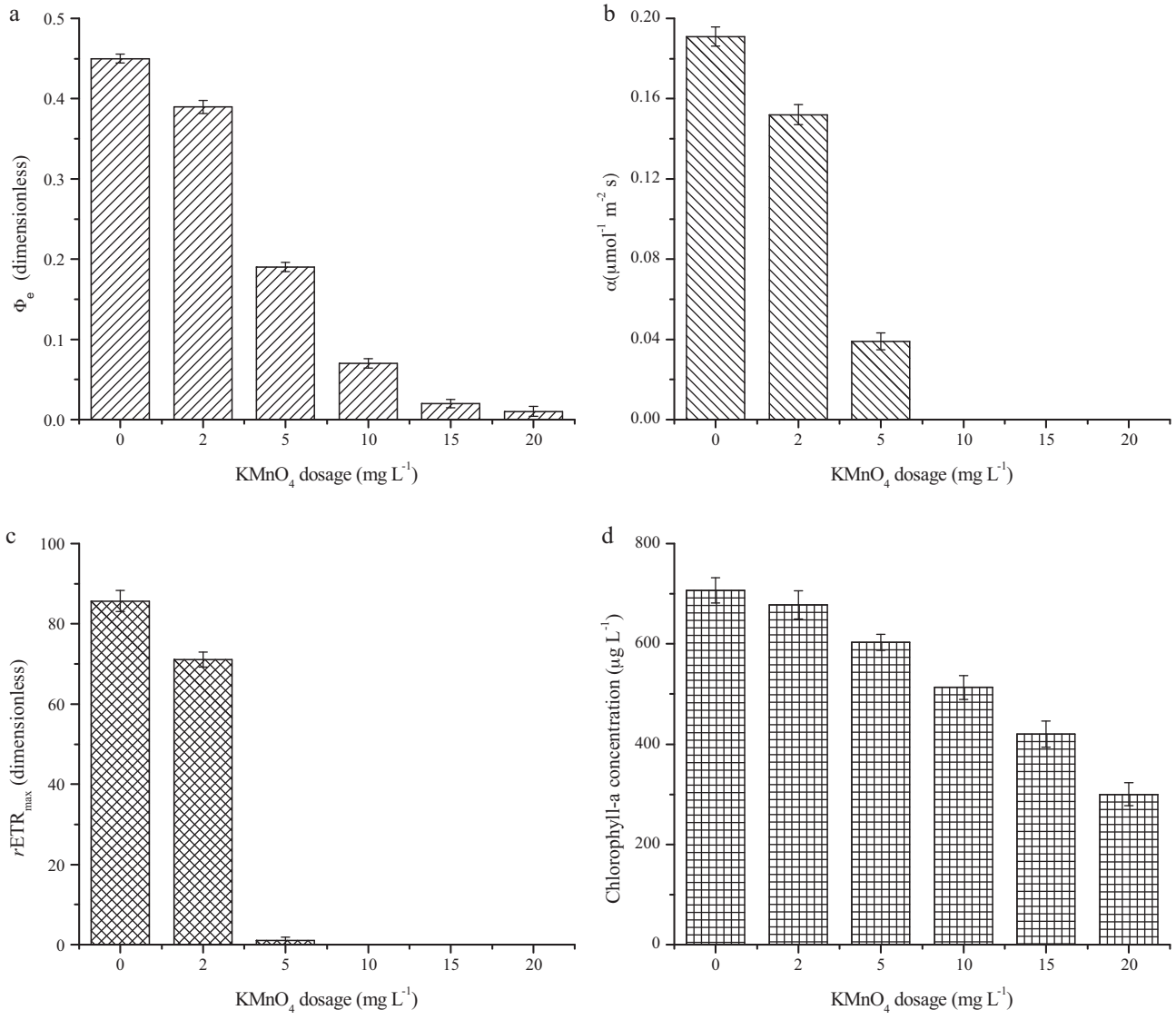

Fig. 1. Photosynthetic parameters of *M. aeruginosa* exposed to various dosages $KMnO_4$: (a) Φ_e, effective quantum yield, dimensionless, (b) α, photosynthetic efficiency, μmol electrons m^{-2} s^{-1}/μmol photons m^{-2} s^{-1}, (c) rETR$_{max}$, maximal electron transport rate, μmol m^{-2} s^{-1}, (d) concentration of *in vivo* chlorophyll-a, μg L^{-1}. Data are the means of three independent samples; error bars indicate the maximum and minimum values of each data set.

dimensionless [22]. It can give a measure of the rate of linear electron transport and so an indication of overall photosynthesis [18]. The photosynthetic parameter α represents the maximum rate of increase of light-limited photosynthesis with a unit of μmol electrons m^{-2} s^{-1}/μmol photons m^{-2} s^{-1}, while rETR$_{max}$ indicates the maximum photosynthetic capacity with a unit of μmol m^{-2} s^{-1} [23]. When the $KMnO_4$ dosages went up from 0 to 10 mg L^{-1}, Φ_e, α, and rETR$_{max}$ decreased from 0.45 to 0.07, from 0.19 to 0 μmol electrons m^{-2} s^{-1}/μmol photons m^{-2} s^{-1}, and from 85.7 to 0 μmol m^{-2} s^{-1}, respectively (Fig. 1a–c). Two-way ANOVA analysis revealed that the differences were significant ($p < 0.001$ among different dosages $KMnO_4$ treated samples). Reduction of these parameters reflected a compromise of the photosynthetic capacity, likely due to the suppression of photosynthesis primary reactions in *M. aeruginosa* cells. Of note, the concentration of chlorophyll-a decreased from 706.5 to 301.6 μg L^{-1} when the $KMnO_4$ dosage increased from 0 to 20 mg L^{-1} (Fig. 1d), suggesting that chlorophyll-a was resistant to $KMnO_4$ oxidation.

3.2. Long-term impact on photosynthetic capacity of cultivated samples

Six-day variations of the photosynthetic parameters for the samples treated by different dosages $KMnO_4$ are presented in Fig. 2. As shown in Fig. 2a, high photosynthetic activity was observed in control cells (no $KMnO_4$ oxidation) and the cells after 2 h low dosages $KMnO_4$ oxidation (2 and 5 mg L^{-1}). The Φ_e of control sample gradually increased from 0.45 to 0.52 within 6-d cultivation, while the ones of samples suffered 2 and 5 mg L^{-1} $KMnO_4$ oxidation initially decreased to 0.39 and 0.19 after 2 h oxidation, then increased to 0.50 and 0.46, respectively. On the contrary, the Φ_e values of higher $KMnO_4$ dosages (≥10 mg L^{-1}) treated samples all decreased to ~0 at 2 d. Similar variation tendencies can be observed in the results of α and rETR$_{max}$ (Fig. 2b and c). During a 6-d cultivation, α and rETR$_{max}$ of the control sample increased from 0.19 to 0.21 μmol electrons m^{-2} s^{-1}/μmol photons m^{-2} s^{-1}, and from 85.7 to 143.7 μmol m^{-2} s^{-1},

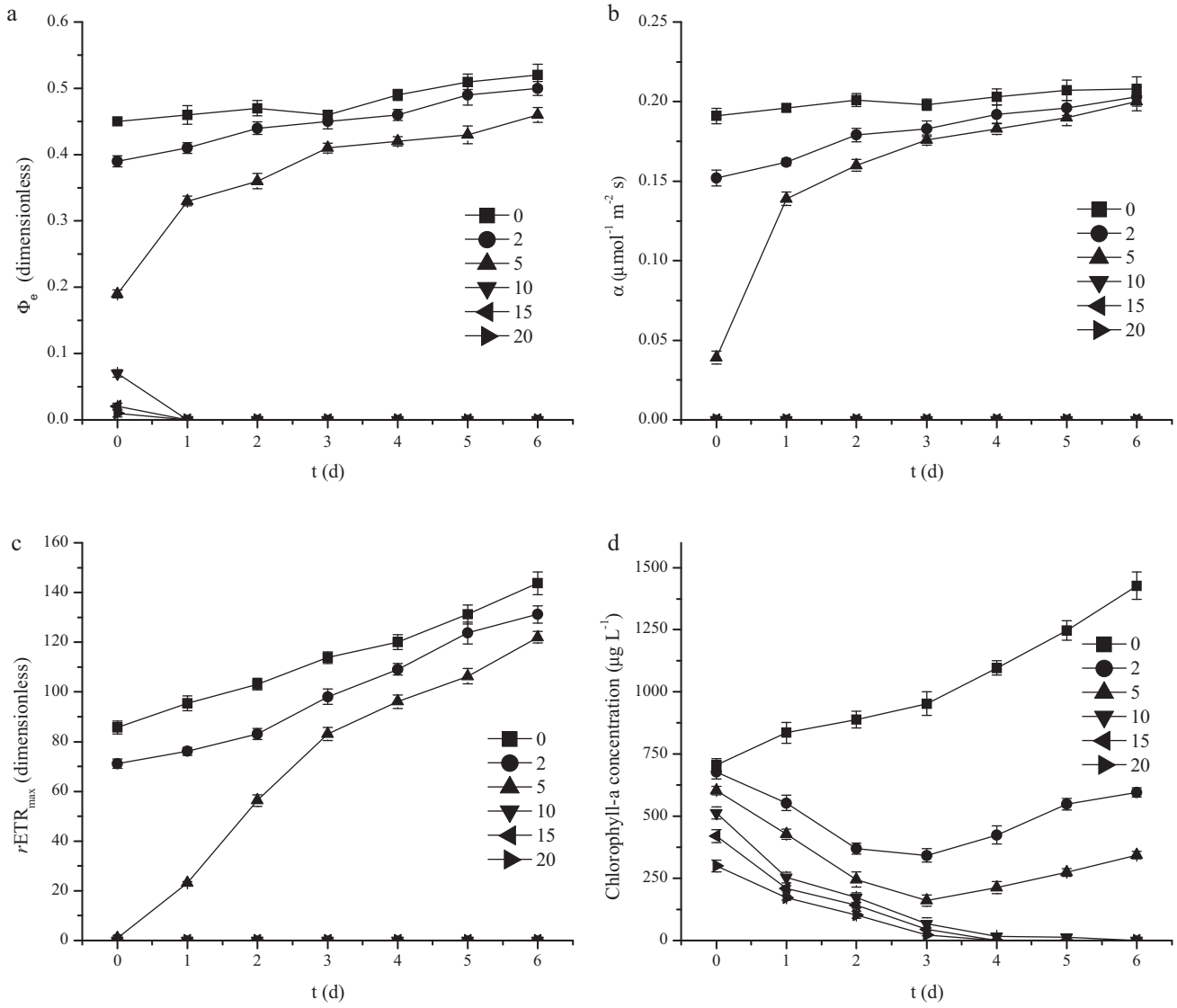

Fig. 2. Photosynthetic parameters of control and $KMnO_4$ treated samples during 6-d cultivation: (a) Φ_e, effective quantum yield, dimensionless, (b) α, photosynthetic efficiency, μmol electrons m^{-2} s^{-1}/μmol photons m^{-2} s^{-1}, (c) $rETR_{max}$, maximal electron transport rate, μmol m^{-2} s^{-1}, (d) concentration of *in vivo* chlorophyll-a, μg L^{-1}. Data are the means of three independent samples; error bars indicate the maximum and minimum values of each data set. Legends represent the $KMnO_4$ dosages. Unit is mg L^{-1}.

respectively. For the samples treated by 2 mg L^{-1} $KMnO_4$ oxidation, they went up from 0.152 to 0.203 μmol electrons m^{-2} s^{-1}/μmol photons m^{-2} s^{-1}, and from 71.1 to 131.2 μmol m^{-2} s^{-1}, respectively, in 6-d cultivation. Similar increasing patterns can be observed in the sample treated by 5 mg L^{-1} $KMnO_4$ oxidation. However, the α and $rETR_{max}$ of higher $KMnO_4$ dosages treated samples (>5 mg L^{-1}) maintained at ~0 during 6-d cultivation. Two-way ANOVA analysis revealed that the differences were significant ($p < 0.001$ among different dosages $KMnO_4$ treated samples). Given that all these photosynthetic parameters were associated with the photosynthetic capacity, these findings demonstrated that certain dosage $KMnO_4$ (>5 mg L^{-1}) can effectively ruin the photosynthesis system, resulting in a decline of activity of *M. aeruginosa* cells. As seen in Fig. 2d, the concentration of chlorophyll-a increased from 706.5 to 1426.7 μg L^{-1} in the control sample. However, the chlorophyll-a of 2 and 5 mg L^{-1} $KMnO_4$ treated samples gradually decreased to 341.8 and 160.6 μg L^{-1} within initial 4-d cultivation, and then increased to 595.3 and 343.0 μg L^{-1}, respectively, at 6 d. These results implied that low dosage $KMnO_4$ oxidation had short-term suppression on the reproduction of *M. aeruginosa*. The concentration of chlorophyll-a in higher dosage $KMnO_4$ treated samples gradually decreased to ~0 μg L^{-1} within 6 d, indicating the decline of intracellular pigments and death of *M. aeruginosa* cells.

3.3. Immediate impacts on the intracellular pigments and cell integrity

Scatter diagrams were plotted to obtain an overview of the cell number, fluorescence characteristic and cell size of *M. aeruginosa* cells. Fig. 3a–f presents the changes of FLR responsivity and FWS responsivity of control and $KMnO_4$ treated *M. aeruginosa* samples. The FLR responsivity represents the amount of intracellular pigments in a single cell (statistical data can be seen in Fig. 3g), while FWS responsivity indicates the cell size. It can be seen that FLR responsivity decreased, while the cells tended to disperse to lower FWS responsivity region. The effects of $KMnO_4$ dosage on cell integrity, as represented by cell diameter and cell density, are presented in Fig. 3h and i, respectively. The average FLR responsivity gradually decreased from 22.8 to 3.4 mV with the increasing $KMnO_4$ dosage from 0 to 20 mg L^{-1}. However, the average cell

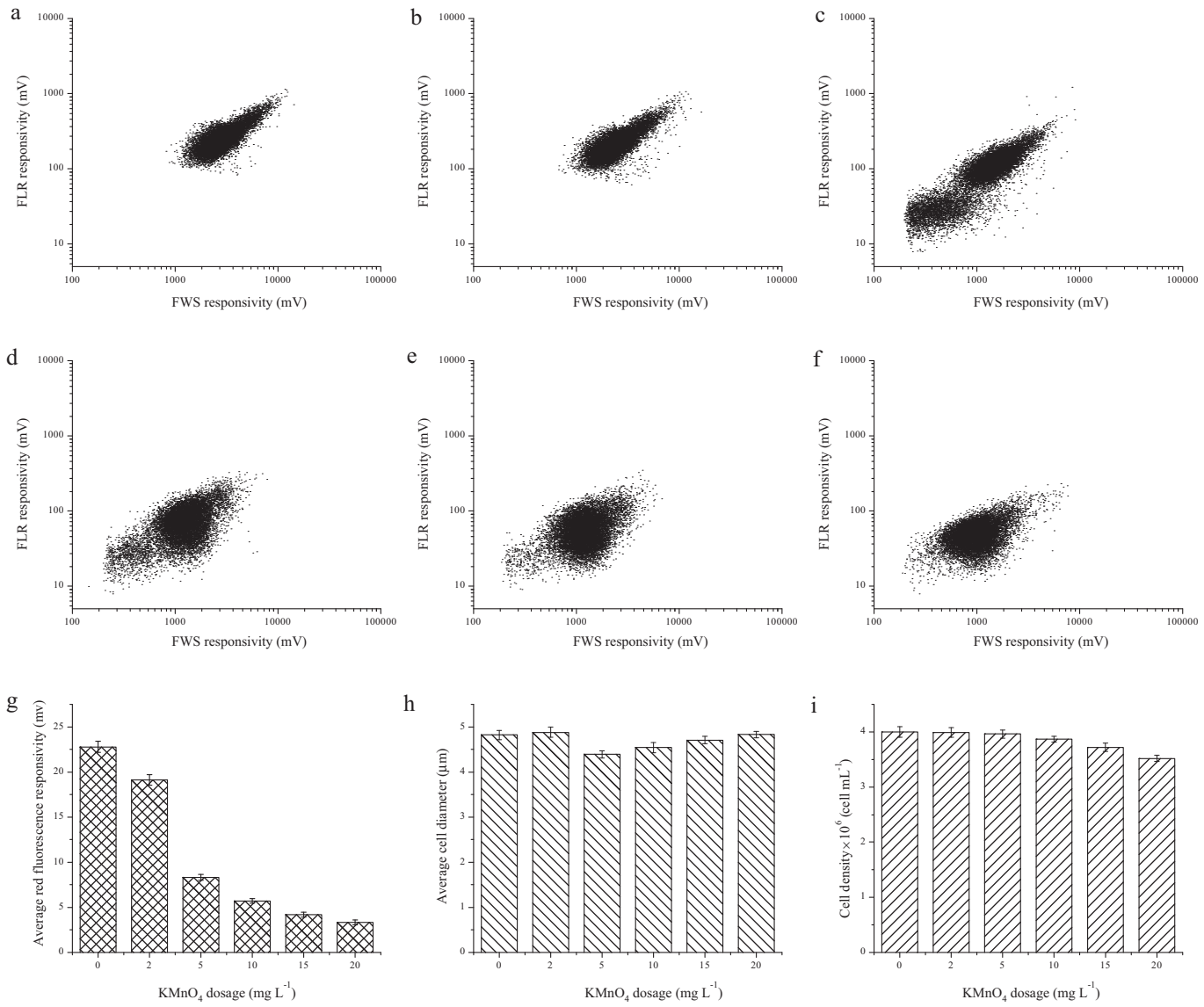

Fig. 3. Two-dimensional scatter diagrams and flow cytometry parameters of *M. aeruginosa* exposed to various dosages $KMnO_4$ at 0 d: (a) before oxidation, (b) 2 mg L^{-1}, (c) 5 mg L^{-1}, (d) 10 mg L^{-1}, (e) 15 mg L^{-1}, (f) 20 mg L^{-1}, (g) average red fluorescence responsivity, mV, (h) average cell diameter, μm, (i) cell density, $\times 10^6$ cells mL^{-1}. Data are the means of three independent samples; error bars indicate the maximum and minimum values of each data set.

diameter (calculated from FWS using CytoClus 3) slightly decreased from 4.8 to 4.4 μm with the increasing $KMnO_4$ dosage from 0 to 5 mg L^{-1}, and then increased to 4.8 μm after 20 mg L^{-1} $KMnO_4$ oxidation. Furthermore, the cell density declined from 4.0×10^6 to 3.5×10^6 cells mL^{-1} with the $KMnO_4$ dosage increased from 0 to 20 mg L^{-1}. Two-way ANOVA analysis revealed that the differences were significant ($p < 0.05$ among different dosages $KMnO_4$ treated samples).

The slight changes of the average cell diameter and cell density after $KMnO_4$ oxidation indicated that the integrity of cells was preserved. However, the significant decrease of the FLR responsivity implied that $KMnO_4$ preferentially ruined the intracellular pigments. Various pigments, *e.g.* chlorophyll-a and phycocyanin, play important roles in photosynthetic processes. Therefore, $KMnO_4$ induced critical damage on the photosynthetic system of *M. aeruginosa*. The results in Sections 3.1 and 3.2 also demonstrated that the photosynthetic capacity of cells was seriously impaired. For example, the photosynthetic parameters of 5 mg L^{-1} $KMnO_4$ treated sample all declined to low levels (Φ_e at 0.19, α at 0.04 μmol electrons m^{-2} s^{-1}/μmol photons m^{-2} s^{-1} and $rETR_{max}$ at 1.1 μmol m^{-2} s^{-1}). At the same time, the cell diameter and cell density slightly declined to 4.4 μm (Fig. 3h) and 3.9×10^6 cells mL^{-1} (Fig. 3i), respectively. This indicated that *M. aeruginosa* cells might be intact, but had low photosynthetic activity and growth potential after proper dosage (5 mg L^{-1}) $KMnO_4$ oxidation.

3.4. Long-term impacts on cell density, intracellular pigments and cell integrity

Impairment on the photosynthetic systems can inhibit the reproduction and recovery of *M. aeruginosa* cells during a long-term cultivation. A typical variation process of the sample treated by 5 mg L^{-1} $KMnO_4$ is presented in Fig. 4. It can be observed that the FLR and FWS significantly changed during 6-d cultivation. Furthermore, the statistical data of all cultivated samples are presented in Fig. 5. The cell density of control sample increased from 4.0×10^6 to 8.3×10^6 cells mL^{-1} within 6 d, indicating that the cells were under an exponential phase (Fig. 5a). The cell density of samples treated by 2 and 5 mg L^{-1} $KMnO_4$ oxidation decreased from 3.9×10^6

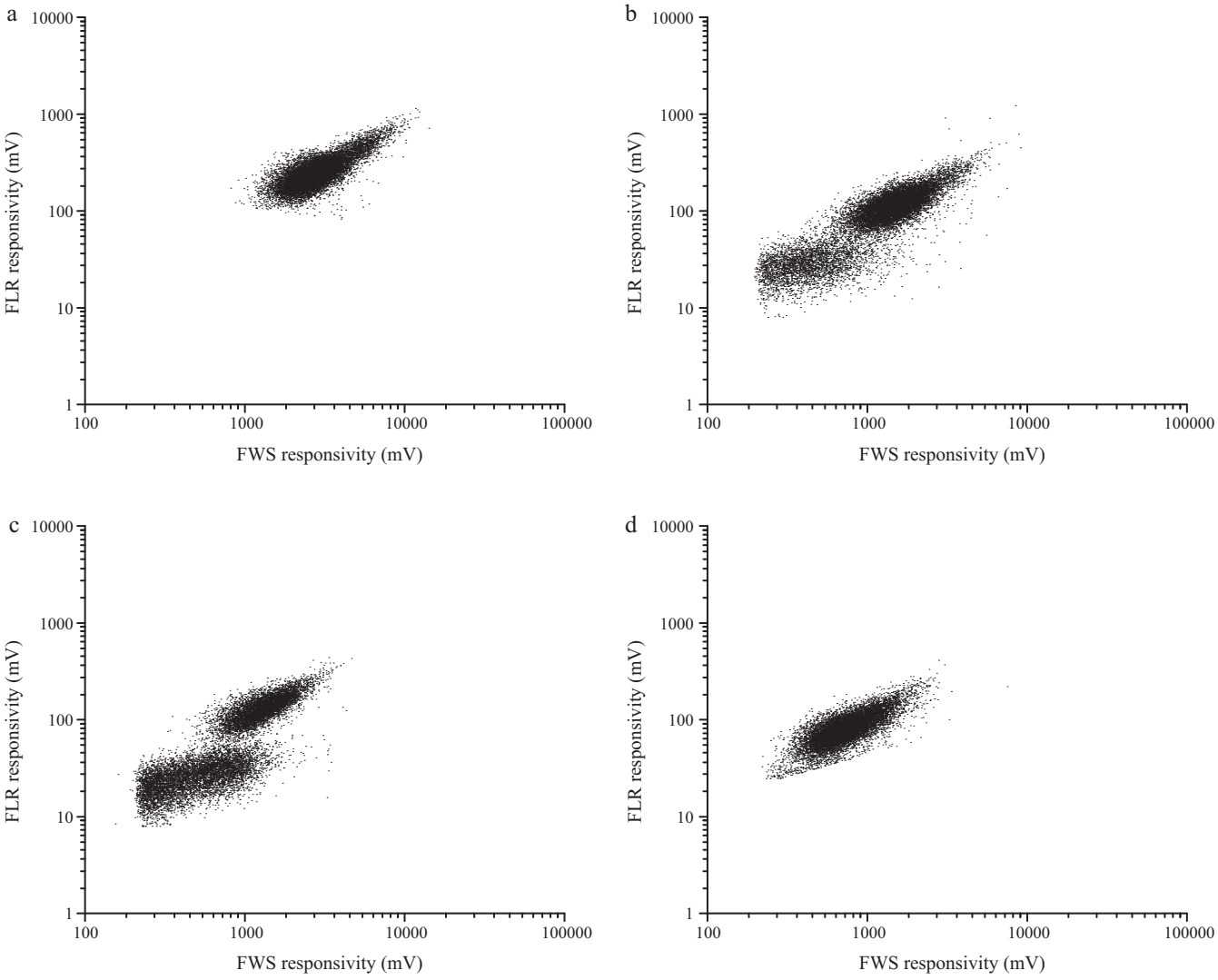

Fig. 4. Two-dimensional scatter diagrams of cultivated *M. aeruginosa* after 5 mg L^{-1} $KMnO_4$ oxidation: (a) before oxidation, (b) 2 d after oxidation, (c) 4 d, (d) 6 d.

to 3.1×10^6 cells mL^{-1} and from 3.9×10^6 to 0.6×10^6 cells mL^{-1} within 4 d, and then increased to 3.4×10^6 and 0.9×10^6 cells mL^{-1}, respectively, at 6 d. Furthermore, after higher dosage $KMnO_4$ oxidation, cell density decreased to 0 within 2-d cultivation. Two-way ANOVA analysis revealed that the differences were significant ($p < 0.001$ among different dosages $KMnO_4$ treated samples). Of note, cell settling was observed during the cultivation (data not showed). These results indicated that $KMnO_4$ oxidation not only inhibited the growing tendency, but also induced cell settling of *M. aeruginosa*.

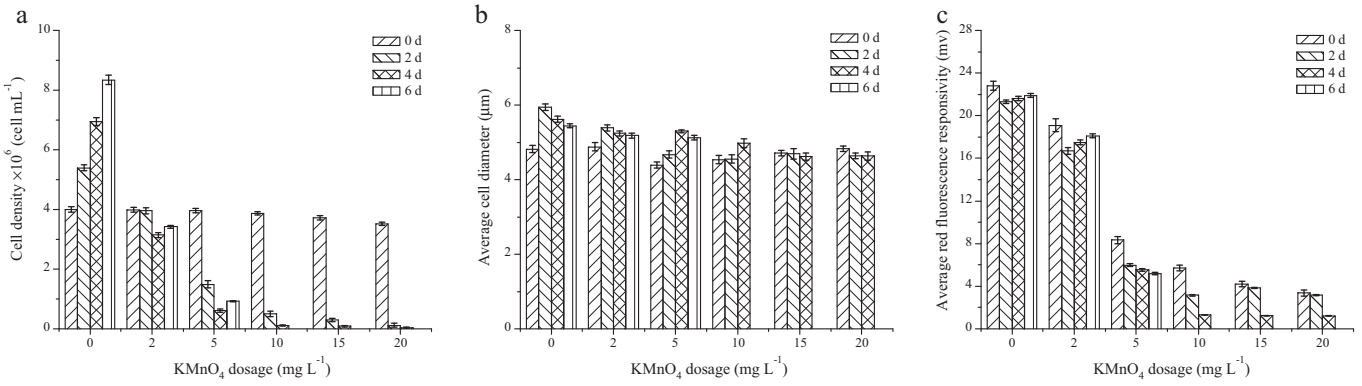

Fig. 5. Statistical data of control and $KMnO_4$ treated samples during 6-d cultivation: (a) cell density, $\times 10^6$ cells mL^{-1}, (b) average cell diameter, μm, (c) average red fluorescence responsivity, mV. Data are the means of three independent samples; error bars indicate the maximum and minimum values of each data set. Legends represent the sampling date.

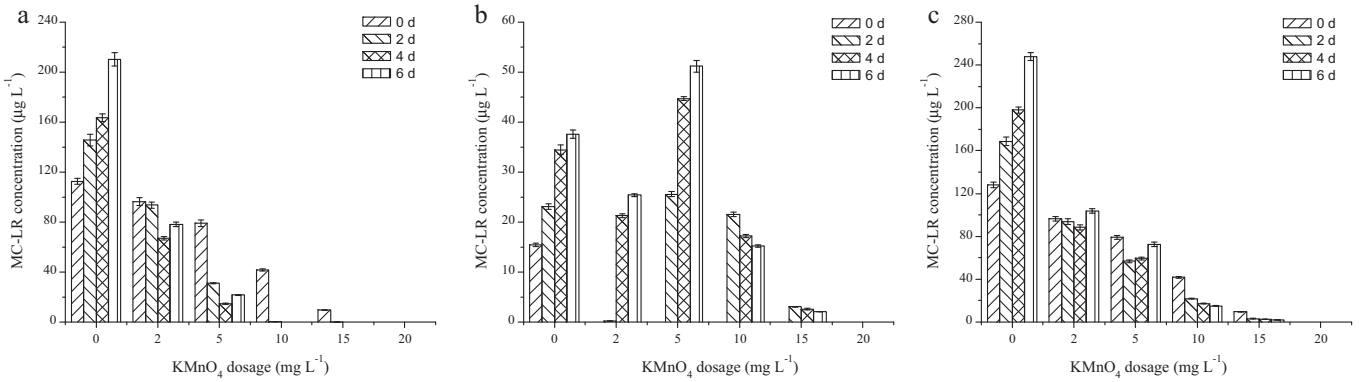

Fig. 6. MC-LR concentration of control and $KMnO_4$ treated samples during 6-d cultivation: (a) intracellular MC-LR, (b) extracellular MC-LR, (c) total MC-LR. Data are the means of three independent samples; error bars indicate the maximum and minimum values of each data set. Legends represent the sampling date.

In the control sample, the average cells diameter developed from 4.8 μm at the beginning, to 5.9 μm at 2 d, and then back to 5.4 μm at 6 d (Fig. 5b). This variation could be explained by the growth of cells. While the *M. aeruginosa* cells were spiked into a new cultivated medium, cell division was prosperous. Conjoined cells might become a larger portion in suspension, resulting in an increase of average cell diameter within 2 d. As cell division slowed down, the cell diameter also decreased. Similar phenomena could be seen in the samples treated by 2 and 5 mg L^{-1} $KMnO_4$, with smaller maximum average cell diameters at 5.4 μm and 5.3 μm, respectively. Particularly, the average cell diameters of samples treated by higher dosages $KMnO_4$ oxidation (>5 mg L^{-1}) were steady until all cells ruptured at 6 d. Two-way ANOVA analysis revealed that the differences were significant ($p < 0.05$ among different dosages $KMnO_4$ treated samples).

The variations of the FLR responsivity are presented in Fig. 5c. The average FLR responsivities of control and 2 mg L^{-1} $KMnO_4$ treated samples initially decreased from 22.8 to 21.3 mV and from 19.1 to 16.7 mV within 2 d, and then increased to 21.9 and 18.1 mV at 6 d, respectively. These findings also ascribed to the prosperous cytoplasmic inclusion accumulation during the cell division phase of *M. aeruginosa*. Moreover, the average FLR of 5 mg L^{-1} $KMnO_4$ treated sample gradually decreased from 8.3 to 5.2 mV within 6-d cultivation, while the ones of higher dosages $KMnO_4$ all decreased to ~0 at 6 d. Two-way ANOVA analysis revealed that the differences were significant ($p < 0.001$ among different dosages $KMnO_4$ treated samples).

3.5. Intracellular and extracellular MC-LR

MC-LR concentrations in the control and $KMnO_4$ treated samples during cultivation are presented in Fig. 6. The intracellular and extracellular MC-LR of control sample increased from 112.6 to 210.1 μg L^{-1} and from 15.4 to 37.6 μg L^{-1}, respectively, in 6 d. On one hand, the intracellular MC-LR declined to different degrees after various dosages $KMnO_4$ oxidation (Fig. 6a). The intracellular MC-LR decreased to 96.4 and 79.1 μg L^{-1} after 2 and 5 mg L^{-1} $KMnO_4$ treatment, and then decreased to 67.2 and 14.7 μg L^{-1}, respectively, within 4-d cultivation. The final concentrations of intracellular MC-LR in these two samples increased to 78.3 and 21.6 μg L^{-1} at 6 d. Furthermore, after higher dosages $KMnO_4$ oxidation (>5 mg L^{-1}), the intracellular MC-LR all decreased to approximate 0 μg L^{-1} at 2 d. On the other hand, the extracellular MC-LR was absent after various dosages $KMnO_4$ treatments (Fig. 6a). In 6-d cultivation, extracellular MC-LR of 2 and 5 mg L^{-1} $KMnO_4$ treated samples gradually increased to 25.4 and 51.2 μg L^{-1}, respectively. However, after 10 and 15 mg L^{-1} $KMnO_4$ oxidation, extracellular MC-LR initially increased to 21.6 and 3.1 μg L^{-1}, and then gradually decreased to 15.2 and 2.1 μg L^{-1}, respectively.

Fig. 6c demonstrates the variations of total MC-LR concentration. Increasing profile of MC-LR can be observed in the control sample during 6-d cultivation. The total MC-LR concentration of 2 mg L^{-1} treated sample gradually decreased from 96.4 to 88.5 μg L^{-1} within 4 d cultivation, and then increased to 103.7 μg L^{-1} at 6 d. The one of 5 mg L^{-1} treated sample demonstrated a similar pattern. However, the MC-LR of samples suffered higher dosages $KMnO_4$ (10 and 15 mg L^{-1}) dramatically declined within 2 d and then presented a slow decrease in remaining 4 d cultivation. Of note, the MC-LR was completely degraded after 20 mg L^{-1} $KMnO_4$ oxidation. Two-way ANOVA analysis revealed that the differences were significant ($p < 0.05$ among different dosages $KMnO_4$ treated samples).

4. Discussion

4.1. Predictability of photosynthetic parameters

Exposure of cells to low levels of physical and chemical stress have been known to trigger apoptosis-like conditions in a variety of photosynthetic organisms, including vascular plants [24,25], unicellular chlorophytes [26], and cyanobacteria [27]. Especially, $KMnO_4$ oxidation was critical harmful to the oxygenic photosynthetic systems of cyanobacteria. The initial energy conversion and electron transfer in these systems are the so-called photosynthesis primary reaction which can be monitored by PAM. The results demonstrated that photosynthetic capacity all decreased to low levels (Φ_e at 0.19, α at 0.04 μmol electrons m^{-2} s^{-1}/μmol photons m^{-2} s^{-1} and $rETR_{max}$ at 1.1 μmol m^{-2} s^{-1}, Fig. 1) after 5 mg L^{-1} $KMnO_4$ oxidation. Φ_e is considered to be proportional to the quantum yield of electron transfer process in photosynthetic systems [28]. Its decrease after $KMnO_4$ oxidation might be associated with the impairments of light harvesting capacity and the retardation of electron transfer, which could further induce suppression of the subsequent stages of photosynthesis. The parameter α represents the maximum rate of the increase of light-limited photosynthesis, and quantifies the efficiency of light capture [29]. Its decline also inferred that $KMnO_4$ oxidation seriously ruined the photosynthetic systems, inhibited the energy transfer and trapping capacity. This finding was also supported by the $rETR_{max}$, which is determined when the rate of photosynthesis is limited by the activity of the electron transport chain or Calvin cycle enzymes [19]. In photosynthesis primary reaction, subunit PS II plays a critical part in electron transport, thus the decrease of $rETR_{max}$ also suggested that the electron transport ability of PS II was impaired by $KMnO_4$ oxidation.

The decrease of photosynthetic parameters indicated the decline of *M. aeruginosa* activity. Low activity might result in suppression of growth and survival. Since the photosynthetic primary reaction is the source of energy in the whole photosynthesis and metabolism, the deprivation of this reaction would result in a lack of energy source, finally death and lysis of *M. aeruginosa* cells. It was verified by the decrease of cell density from 4.0×10^6 to 0.6×10^6 cells mL^{-1} within 4-d cultivation after 5 mg L^{-1} $KMnO_4$ oxidation (Fig. 5a). This delayed decline of cell density might be due to the store of energy source, *e.g.* polysaccharide and protein, in *M. aeruginosa* cells. However, the photosynthetic capacities all dramatically recovered (Φ_e at 0.42, α at 0.18 μmol electrons m^{-2} s^{-1}/μmol photons m^{-2} s^{-1} and $rETR_{max}$ at 96.1 μmol m^{-2} s^{-1}, Fig. 2) at 4 d, and the cell density increased to 0.9×10^6 cells mL^{-1} at 6 d (Fig. 5a). These results suggested that the photosynthetic parameters obtained from PAM might be potential tools to predict the growth tendency of *M. aeruginosa*. Furthermore, the recoveries of 2 and 5 mg L^{-1} $KMnO_4$ treated samples also indicated that *M. aeruginosa* cells can survive after low dosage $KMnO_4$ oxidation. Given that survived *M. aeruginosa* cells might remain in water treatment facilities (*e.g.* sedimentation basin), an improper dosage $KMnO_4$ pretreatment might have limited efficiency for *M. aeruginosa* and MC-LR elimination in drinking water treatment plants. Of note, the chlorophyll-a concentration of sample treated by 5 mg L^{-1} $KMnO_4$ decreased from 603.1 to 213.3 μg L^{-1} within 4 d, and then increased to 343.2 μg L^{-1} at 6 d. Synchronous variation can be observed in the results of cell density, indicating that chlorophyll-a concentration might be appropriate to monitor the biomass of *M. aeruginosa* cells. Thus, photosynthetic parameters combined with chlorophyll-a concentration can be used as indicators to control the $KMnO_4$ dosage in the pre-oxidation of *M. aeruginosa* contained raw water.

4.2. Cell lysis and MC-LR release risk

Both intracellular and extracellular MC-LR decreased after various dosages $KMnO_4$ oxidation. On one hand, the extracellular MC-LR was absent after $KMnO_4$ oxidation (Fig. 6b), indicating that $KMnO_4$ effectively degraded the extracellular MC-LR in suspension. It was reported that the half-life of MCs under $KMnO_4$ oxidation was less than 1 min in pure water, and more than 99% of MCs was degraded within 10 min [15]. Rodrıgueza et al. also found that $KMnO_4$ was a feasible oxidant for the removal of MCs in solution, but they confirmed that the oxidation might lead to other toxic oxidation products [30]. On the other hand, the concentration of intracellular MC-LR declined from 112.6 to 41.8 μg L^{-1} immediately after 0–10 mg L^{-1} $KMnO_4$ oxidation (Fig. 6a), suggesting that the risk of MC-LR release still existed after low dosage $KMnO_4$ treatment. This was verified by the decrease of biomass and the transfer between intracellular MC-LR and extracellular MC-LR during 6-d cultivation. For example, the cell density decreased from 3.9×10^6 to 0.6×10^6 cells mL^{-1} within 4-d cultivation after 5 mg L^{-1} $KMnO_4$ oxidation (Fig. 5a). Simultaneously, intracellular MC-LR decreased from 79.1 to 14.7 μg L^{-1} and transferred to extracellular MC-LR, which increased from 0 to 44.7 μg L^{-1}. These findings suggested that a critical lysis of *M. aeruginosa* cells after $KMnO_4$ treatment could significantly release intracellular MC-LR. Daly et al. reported that cyanobacteria retain cyanotoxins within their cell structure, and release these toxins into the surrounding water after cell lysis [9]. Furthermore, the increase of cell density to 0.9×10^6 cells mL^{-1} at 6 d indicated a recovery of *M. aeruginosa* and resulted in increases of both fractions of MC-LR. Live *M. aeruginosa* cells can release MC-LR as well, thus the lysis and incomplete inactivation of *M. aeruginosa* cell by low dosage $KMnO_4$ exacerbated the accumulation of MC-LR in suspension, resulting in the highest extracellular concentration of 51.2 μg L^{-1} at 6 d.

5. Conclusions

In this study, the immediate and long-term impacts of $KMnO_4$ oxidation on the cell activity, integrity, recovery and MC-LR release risk of *M. aeruginosa* were investigated. Our results demonstrated that the photosynthetic parameters obtained from PAM were useful tools to predict the lysis and recovery tendency of *M. aeruginosa* cells. $KMnO_4$ oxidation was proven to be effective on *M. aeruginosa* inactivation and MC-LR degradation. However, the $KMnO_4$ dosage was a vital parameter to control the results in current experiment. Low dosage $KMnO_4$ (2–5 mg L^{-1}) oxidation had limited efficiency for intracellular MC-LR degradation and *M. aeruginosa* cells inactivation. In subsequent cultivated experiments, recovery of cells activity and release of MC-LR were observed. Higher dosage $KMnO_4$ ($\geq$10 mg L^{-1}) deprived the cell activity and degraded the extracellular MC-LR. However, high dosage $KMnO_4$ might have negative effects on drinking water treatment processes.

In order to obtain safety drinking water from *M. aeruginosa* contained raw water (*e.g.* the raw water of Lake Taihu, China), $KMnO_4$ can be used as a pre-oxidant. However, the dosage of $KMnO_4$ should be considered carefully in practice. Appropriate dosage $KMnO_4$ can deprive the photosynthetic capacity of *M. aeruginosa* cells and degrade the extracellular MC-LR, resulting in low activity but intact cells in suspension. In subsequent treatments (*e.g.* sedimentation or flotation), residual intracellular MC-LR can be removed accompanied with *M. aeruginosa* cells. It should be optimized in practice with regard toward treatment efficiency and combined treatment processes.

Acknowledgments

This project was supported by the National Major Science and Technology Project of China (No. 2008ZX07421-002, 2008ZX07421-004) and the Research and Development Project of Ministry of Housing and Urban-Rural Development of China (No. 2009-K7-4).

References

[1] D.R. de Figueiredo, U.M. Azeiteiro, S.M. Esteves, F.J.M. Goncalves, M.J. Pereira, Microcystin-producing blooms—a serious global public health issue, Ecotoxicol. Environ. Saf. 59 (2004) 151–163.
[2] B.C. Hitzfeld, S.J. Hoger, D.R. Dietrich, Cyanobacterial toxins: removal during drinking water treatment and human risk assessment, Environ. Health Perspect. 108 (2000) 113–122.
[3] J.L. Smith, G.L. Boyer, P.V. Zimba, A review of cyanobacterial odorous and bioactive metabolites: impacts and management alternatives in aquaculture, Aquaculture 280 (2008) 5–20.
[4] R.K. Henderson, A. Baker, S.A. Parsons, B. Jefferson, Characterisation of algogenic organic matter extracted from cyanobacteria, green algae and diatoms, Water Res. 42 (2008) 3435–3445.
[5] J.J. Chen, H.H. Yeh, I.C. Tseng, Effect of ozone and permanganate on algae coagulation removal—pilot and bench scale tests, Chemosphere 74 (2009) 840–846.
[6] H. Sakai, H. Katayama, K. Oguma, S. Ohgaki, Kinetics of *Microcystis aeruginosa* growth and intracellular microcystins release after UV irradiation, Environ. Sci. Technol. 43 (2009) 896–901.
[7] H.F. Miao, W.Y. Tao, The mechanisms of ozonation on cyanobacteria and its toxins removal, Sep. Purif. Technol. 66 (2009) 187–193.
[8] W. Schmidt, H. Willmitzer, K. Bornmann, J. Pietsch, Production of drinking water from raw water containing cyanobacteria—pilot plant studies for assessing the risk of microcystin breakthrough, Environ. Toxicol. 17 (2002) 375–385.
[9] R.I. Daly, L. Ho, J.D. Brookes, Effect of chlorination on *Microcystis aeruginosa* cell integrity and subsequent microcystin release and degradation, Environ. Sci. Technol. 41 (2007) 4447–4453.
[10] L.A. Lawton, P.K.J. Robertson, Physico-chemical treatment methods for the removal of microcystins (cyanobacterial hepatotoxins) from potable waters, Chem. Soc. Rev. 28 (1999) 217–224.
[11] J. Ma, G.B. Li, Laboratory and full-scale plant studies of permanganate oxidation as an aid in coagulation, Water Sci. Technol. 27 (1993) 47–54.

[12] J.J. Chen, H.H. Yeh, The mechanisms of potassium permanganate on algae removal, Water Res. 39 (2005) 4420–4428.
[13] S.C. Tung, T.F. Lin, C.L. Liu, S.D. Lai, The effect of oxidants on 2-MIB concentration with the presence of cyanobacteria, Water Sci. Technol. 49 (2004) 281–288.
[14] E. Rodriguez, M.E. Majado, J. Meriluoto, J.L. Acero, Oxidation of microcystins by permanganate: reaction kinetics and implications for water treatment, Water Res. 41 (2007) 102–110.
[15] X.G. Chen, B.D. Xiao, J.T. Liu, T. Fang, X.Q. Xu, Kinetics of the oxidation of MCRR by potassium permanganate, Toxicon 45 (2005) 911–917.
[16] S. Bailey, A. Grossman, Photoprotection in cyanobacteria: regulation of light harvesting, Photochem. Photobiol. 84 (2008) 1410–1420.
[17] D. Campbell, V. Hurry, A.K. Clarke, P. Gustafsson, G. Oquist, Chlorophyll fluorescence analysis of cyanobacterial photosynthesis and acclimation, Microbiol. Mol. Biol. Rev. 62 (1998) 667–683.
[18] K. Maxwell, G.N. Johnson, Chlorophyll fluorescence—a practical guide, J. Exp. Bot. 51 (2000) 659–668.
[19] P.J. Ralph, R. Gademann, Rapid light curves: a powerful tool to assess photosynthetic activity, Aquat. Bot. 82 (2005) 222–237.
[20] M. Thyssen, B. Beker, D. Ediger, D. Yilmaz, N. Garcia, M. Denis, Phytoplankton distribution during two contrasted summers in a Mediterranean harbour: combining automated submersible flow cytometry with conventional techniques, Environ. Monit. Assess. 173 (2011) 1–16.
[21] J.Z. Chen, J. Dai, H.Y. Zhang, C.Y. Wang, G.Q. Zhou, Z.P. Han, Z.L. Liu, Bioaccumulation of microcystin and its oxidative stress in the apple (*Malus pumila*), Ecotoxicology 19 (2010) 796–803.
[22] B. Genty, J.M. Briantais, N.R. Baker, The relationship between the quantum yield of photosynthetic electron transport and quenching of chlorophyll fluorescence, Biochim. Biophys. Acta 990 (1989) 87–92.
[23] S. Ihnken, A. Eggert, J. Beardall, Exposure times in rapid light curves affect photosynthetic parameters in algae, Aquat. Bot. 93 (2010) 185–194.
[24] E. Lam, O. del Pozo, Caspase-like protease involvement in the control of plant cell death, Plant Mol. Biol. 44 (2000) 417–428.
[25] E. Lam, N. Kato, M. Lawton, Programmed cell death, mitochondria and the plant hypersensitive response, Nature 411 (2001) 848–853.
[26] J.A. Berges, P.G. Falkowski, Physiological stress and cell death in marine phytoplankton: Induction of proteases in response to nitrogen or light limitation, Limnol. Oceanogr. 43 (1998) 129–135.
[27] I. Berman-Frank, K.D. Bidle, L. Haramaty, P.G. Falkowski, The demise of the marine cyanobacterium, *Trichodesmium* spp., via an autocatalyzed cell death pathway, Limnol. Oceanogr. 49 (2004) 997–1005.
[28] H. Dau, Molecular mechanisms and quantitative models of variable photosystem-II fluorescence, Photochem. Photobiol. 60 (1994) 1–23.
[29] M.J. Behrenfeld, O. Prasil, M. Babin, F. Bruyant, In search of a physiological basis for covariations in light-limited and light-saturated photosynthesis, J. Phycol. 40 (2004) 4–25.
[30] E.M. Rodriguez, J.L. Acero, L. Spoof, J. Meriluoto, Oxidation of MC-LR and -RR with chlorine and potassium permanganate: toxicity of the reaction products, Water Res. 42 (2008) 1744–1752.